Available on CMS information server

CMS NOTE 2010/998

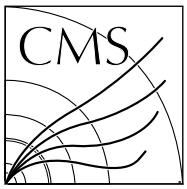

The Compact Muon Solenoid Experiment

CMS Note

Mailing address: CMS CERN, CH-1211 GENEVA 23, Switzerland

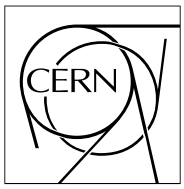

December 3, 2010

Z candle note

A. Author, B. Author, C. Author

CERN, Geneva, Switzerland

D. Author, E. Author, F. Author

Institute of Experimental Physics, Hepcity, Wonderland

CMS collaboration

Abstract

1 Introduction

The CMS detector in LHC is well-suited to measure muon with high reconstruction efficiency. Especially in the dimuon channel of Z0 boson production one can get a very clean signal. Owing to good coverage of the detector, Z0 in the muon channel can act as a good handle on probing various quantities and to provide a data-driven way to estimate for example reconstruction and trigger efficiencies. In events where the Z0 boson is recoiling against other objects, the energy scale of the recoiling object can be calibrated by the precise measurement of the momentum of Z0.

Z0 boson in association with jet production events is an example of utilizing the clean signature of Z0 boson to probe quantities related to jets. The multiplicity of jets is expected to follow an exponential relation, roughly due to the fact that there is one more strong vertex in the diagrams. Previous experiments (TODO: INSERT CITATION) have verified the exponential relation, and results from the LHC with 7TeV CM energy can provide more insight in the underlying physics.

The study from Z0 boson in muon channel in association with jet production can also be used to study important background in many beyond standard model searches, since the kinematics is very similar in the muon channel and in the neutrino channels. The knowledge of the branching ratios together with various distributions from Z to dimuons gives us an estimate of the irreducible background.

Goal of this study. (TODO)

In section 1, section 2, section 3, etc. (TODO: FILL THIS IN LATER)

2 MC samples and data used

All Monte-Carlo samples are fully-simulated with the CMS detector. The signal sample, Z0 to leptons with jet production, is generated by MADGRAPH generator. Background processes such as W boson (to leptons) with jet production and ttbar with jets are also generated by MADGRAPH. QCD background is generated by PYTHIA6 generator, requiring at least two muons. The samples used are summarized in table 1

Table 1: MC samples used.

MC	Cross section	Generator	Generator-level cut
$Z \to ll$ + Jets	2400pb	MADGRAPH	$m_{l\bar{l}} > 50GeV/c^2$
$W \to l\nu_l$ + Jets	24170pb	MADGRAPH	
$t\bar{t}$ + Jets	95pb	MADGRAPH	
QCD (with two muons)	48.44mb * 0.0000112	PYTHIA6	

Proton-proton collision data collected in 2010 are used. Both run 2010A and run 2010B data are combined to include as much statistics as possible. The run ranges and datasets used are summarized in table 2

Table 2: Data samples (TODO: CALCULATE LUMINOSITY)

Run range	dataset	integrated luminosity
135821-144114	/Mu/Run2010A-Sep17ReReco_v2	
146240-149442	/Mu/Run2010B-PromptReco_v2	

3 Selection criteria

3.1 Triggers

Since the instantaneous luminosity was increasing exponentially during the course of 2010, the corresponding high-level trigger menu keeps changing. In particular, some of the muon triggers with lower PT threshold got prescaled in later runs. In each run range, the lowest unprescaled HLT trigger is used. The triggers used in different run ranges are summarized in table 3. We require a high enough momentum muon as requirement of one of the muon from Z decay, and the triggers are efficient in the ranges we are interested in, no matter which trigger is used.

Table 3: Lowest unprescaled trigger in different run ranges (TODO: FILL ME IN)

Run range	Lowest unprescaled trigger
135821-147116	HLT_Mu9
147196-148058	HLT_Mu11
148819-149442	HLT_Mu15

3.2 Muon selection

To ensure that all possible data is included, a minimum selection is applied to select muons as candidates from Z decay. The following list of variables are used in the identification of candidate muons:

1. Muon type. The muons to be considered a candidate needs to be both a tracker muon (inside out) and a global muon (outside in).
2. Number of valid hits in pixel and strip tracker system. We require that there is at least one hit in any of the pixel detector layers, as well as a total of 6 hits in both pixel and silicon strip detectors combined.
3. Valid hit in the muon chambers. At least one valid hit in the muon chambers that is consistent with the global muon track fitting is required.
4. The reduced chi2 in the global muon track fitting is required to be less than 10.
5. Isolation. We require that the combined relative isolation is smaller than 30% in a cone size of 0.3. This is not required to obtain a high purity sample, but rather that we want to have a data-driven background control sample. Muons from Z decay a priori do not have a preference in terms of isolation with respect to other activities in the events, but in background events muons are mostly produced in jets and therefore have bad isolations.

In addition to the muon identification criteria, the following kinematic constraints are required:

1. For the "first leg" (harder) muon, we require PT greater than 15 GeV/c, and pseudorapidity range between -2.1 and 2.1.
2. The PT requirement of the other muon (softer, "second leg") is 10 GeV/c, and a slightly larger η range between -2.4 and 2.4.

3.3 Z selection

In addition to the muon identification and kinematics criteria, the muon pair is required to be at least 0.01 units apart in $\eta - \phi$ space to reject possible doubly-reconstructed muons. Any muon pairs with invariant mass between 60-120 GeV/c^2 are considered a good Z0 candidate. When there are more than one candidates in the event, the candidate with highest transverse momentum is used.

3.4 Jet reconstruction and selection

A number of different jet reconstruction algorithms are considered in this study in order to demonstrate that the scaling is not a coincidence of certain sub-detectors.

1. Calorimetric jet (*CaloJet*). The jet constituents are taken from both hadronic calorimeter deposits and electomagnetic calorimeter deposits. The calorimeters are first combined into *calotowers* according the the geometrical locations of the cells. Calotowers are then treated as four vector with zero norm to be included in the jet clustering algorithm. The jets need to be corrected for energy. To estimate the effect of the energy correction, we also perform the analysis in terms of uncorrected energies. The threshold for counting CaloJets is 30 GeV/c, while the threshold for couting uncorrected CaloJets is 20 GeV/c.
2. Uncorrected track jet. All tracks that pass some basic quality selection criteria are served as input to the jet clustering algorithm, again treating them as massless. We require that the number of hits along the track is greater than 6, and the normalized χ^2 is smaller than 20. The track vertex, compared to the primary vertex, has to be within 0.1cm in z direction, 0.1 cm in magnitude, and 600 μm in the transverse direction. Also, if

there exists another reconstructed vertex that is closer to the best primary vertex, the track is not included in the jet clustering. The pseudorapidity of the track is required to be $-2.4 < |\eta| < 2.4$, and the momentum is required to be within range 0.5-500 GeV/c. The threshold for track jet counting is 20 GeV/c.

3. Particle flow jet (*PF jet*). There is an elaborate set of algorithms that attempts to reconstruct particle candidates as good as possible, and then to start physics analysis from there. The jet algorithms take in the reconstructed candidates as input. The threshold for PF jet counting is 20 GeV/c. Compatibility with the primary vertex is not implemented yet.

3.5 Selection efficiencies and expected yields

The selection efficiencies for different MC samples are shown in table 4. The expected yields are summaried in table 5 for MC samples for different jet flavors for 10 pb^{-1}. Note that in the QCD sample the statistics is low and nothing is left after all selections.

Signal selection efficiencies as a function of different jet multiplicity events are also calculated and shown in tables 6 and 7. The efficiencies across different jet multiplicity bins are compatible with each other for different selections, except for a few cases. The requirement of two muons which reflects the acceptance due to Z momentum spectrum produces the difference with respect to different jet multiplicities, and also that there might be muons produced in jets. Efficiency from the isolation requirement is also different since when there are more jets in the event, the muons from vector boson is more likely overlapped with any of the jets, hence the smaller selection efficiency. The PT and η requirement is similar across all jet multiplicity bins when there is at least one jet, which is reflective of the fact that when there are recoiling jets, the momentum of Z is generally harder than that in events when there is no recoiling jets.

Table 4: Selection efficiency for signal and background for each applied requirement. The values quoted are computed with respect to the previously-applied selection.

Sample	$Z+jets$	$W+jets$	$t\bar{t}+jets$	QCD
Two Muons	57.78 ± 0.16	4.38 ± 0.01	30.53 ± 0.06	57.84 ± 0.09
Two Global Muons	89.65 ± 0.29	7.28 ± 0.04	40.78 ± 0.12	58.75 ± 0.13
Pixel Hits	99.45 ± 0.33	92.99 ± 0.76	97.46 ± 0.35	95.63 ± 0.23
Tracking Hits	99.95 ± 0.34	97.22 ± 0.81	98.94 ± 0.36	99.11 ± 0.24
Valid Muon Hits	97.40 ± 0.33	67.90 ± 0.64	86.60 ± 0.32	78.34 ± 0.21
Muon χ^2	99.00 ± 0.34	92.39 ± 0.96	95.99 ± 0.38	97.47 ± 0.27
Isolation	96.94 ± 0.33	25.90 ± 0.43	14.49 ± 0.11	28.56 ± 0.12
p_T and $\lvert\eta\rvert$	91.67 ± 0.33	0.55 ± 0.11	32.99 ± 0.49	0.00 ± 0.00
Total	44.12 ± 0.14	0.00 ± 0.00	0.48 ± 0.01	0.00 ± 0.00

4 Fit strategy

4.1 Signal and background shape

The signal PDF is parameterized by a Cruijff function, defined as follows:

$$F_S(M_{ll}; m, \sigma_L, \sigma_R, \alpha_L, \alpha_R) = N_s e^{-\frac{(M_{ll}-m)^2}{2\sigma^2 + \alpha^2(M_{ll}-m)^2}},$$

where $\sigma = \sigma_L(\sigma_R)$ for $M_{ll} < m(M_{ll} > m)$ and $\alpha = \alpha_L(\alpha_R)$ for $M_{ll} < m(M_{ll} > m)$. The background shape is chosen as a falling exponential, as can be seen in the QCD sample which dominates the background in low jet multiplicity bin. When the number of jets is larger, events with $t\bar{t}$ start to have a significant contribution, and those are also well-modeled by a falling exponential. Even though the exponent is not the same in different samples, the exponent is floated in the fit, and the difference in exponent will be taken account for.

4.2 Bias from assuming signal shape with wrong parameters

It is necessary to test whether the signal shape assumption causes any bias on the extracted signal yield. Specifically, if we were to fix any of the parameters in the fit, what is the bias caused by a badly chosen set of parameters.

Table 5: Expected number of events in (2.66 pb^{-1} for signal and background Monte Carlo samples.

Jet Counting	$Z + jets$	$W + jets$	$t\bar{t} + jets$	QCD
PFJets				
$N(\geq 0\ jets)$	938.78 ± 30.64	0.16 ± 0.41	1.21 ± 1.10	0.00 ± 0.00
$N(\geq 1\ jets)$	140.18 ± 11.84	0.03 ± 0.18	1.18 ± 1.09	0.00 ± 0.00
$N(\geq 2\ jets)$	25.05 ± 5.00	0.01 ± 0.11	0.95 ± 0.98	0.00 ± 0.00
$N(\geq 3\ jets)$	4.54 ± 2.13	0.01 ± 0.11	0.41 ± 0.64	0.00 ± 0.00
$N(\geq 4\ jets)$	0.90 ± 0.95	0.00 ± 0.00	0.13 ± 0.36	0.00 ± 0.00
TrackJets				
$N(\geq 0\ jets)$	938.78 ± 30.64	0.16 ± 0.41	1.21 ± 1.10	0.00 ± 0.00
$N(\geq 1\ jets)$	99.29 ± 9.96	0.03 ± 0.18	1.08 ± 1.04	0.00 ± 0.00
$N(\geq 2\ jets)$	13.90 ± 3.73	0.01 ± 0.11	0.67 ± 0.82	0.00 ± 0.00
$N(\geq 3\ jets)$	2.24 ± 1.50	0.00 ± 0.00	0.22 ± 0.47	0.00 ± 0.00
$N(\geq 4\ jets)$	0.35 ± 0.59	0.00 ± 0.00	0.06 ± 0.24	0.00 ± 0.00
CaloJets				
$N(\geq 0\ jets)$	938.78 ± 30.64	0.16 ± 0.41	1.21 ± 1.10	0.00 ± 0.00
$N(\geq 1\ jets)$	211.96 ± 14.56	0.07 ± 0.26	1.19 ± 1.09	0.00 ± 0.00
$N(\geq 2\ jets)$	43.27 ± 6.58	0.03 ± 0.16	1.02 ± 1.01	0.00 ± 0.00
$N(\geq 3\ jets)$	8.63 ± 2.94	0.01 ± 0.11	0.52 ± 0.72	0.00 ± 0.00
$N(\geq 4\ jets)$	1.81 ± 1.35	0.00 ± 0.00	0.21 ± 0.46	0.00 ± 0.00
UncorrectedCaloJets				
$N(\geq 0\ jets)$	938.78 ± 30.64	0.16 ± 0.41	1.21 ± 1.10	0.00 ± 0.00
$N(\geq 1\ jets)$	114.41 ± 10.70	0.05 ± 0.21	1.15 ± 1.07	0.00 ± 0.00
$N(\geq 2\ jets)$	17.73 ± 4.21	0.01 ± 0.08	0.81 ± 0.90	0.00 ± 0.00
$N(\geq 3\ jets)$	2.99 ± 1.73	0.01 ± 0.08	0.30 ± 0.55	0.00 ± 0.00
$N(\geq 4\ jets)$	0.59 ± 0.77	0.00 ± 0.00	0.08 ± 0.29	0.00 ± 0.00

Table 6: Selection efficiency for signal in different calo jet bin for each applied requirement. The values quoted are computed with respect to the previously-applied selection.

Jet count	$\geq 0jets$	$\geq 1jet$	$\geq 2jets$	$\geq 3jets$	$\geq 4jets$
Two Muons	57.78 ± 0.16	69.94 ± 0.41	75.71 ± 0.98	79.17 ± 2.29	80.14 ± 4.99
Two Global Muons	89.65 ± 0.29	89.98 ± 0.59	89.59 ± 1.27	89.95 ± 2.83	88.36 ± 5.99
Pixel Hits	99.45 ± 0.33	99.38 ± 0.67	99.43 ± 1.45	99.38 ± 3.21	99.27 ± 6.95
Tracking Hits	99.95 ± 0.34	99.95 ± 0.67	99.93 ± 1.46	99.84 ± 3.23	100.00 ± 7.01
Valid Muon Hits	97.40 ± 0.33	97.05 ± 0.66	97.06 ± 1.43	97.17 ± 3.17	95.82 ± 6.79
Muon χ^2	99.00 ± 0.34	98.77 ± 0.68	98.66 ± 1.47	98.38 ± 3.24	98.46 ± 7.08
Isolation	96.94 ± 0.33	90.77 ± 0.64	88.05 ± 1.36	85.16 ± 2.94	84.38 ± 6.36
p_T and $\lvert\eta\rvert$	91.67 ± 0.33	89.06 ± 0.66	88.56 ± 1.45	89.90 ± 3.31	90.43 ± 7.29
Total	44.12 ± 0.14	48.44 ± 0.32	50.32 ± 0.74	51.72 ± 1.70	50.60 ± 3.63

Table 7: Selection efficiency for signal in different uncorrected calo jet bin for each applied requirement. The values quoted are computed with respect to the previously-applied selection.

Jet count	$\geq 0jets$	$\geq 1jet$	$\geq 2jets$	$\geq 3jets$	$\geq 4jets$
Two Muons	57.78 ± 0.16	71.88 ± 0.57	77.08 ± 1.55	80.94 ± 4.09	81.76 ± 9.35
Two Global Muons	89.65 ± 0.29	89.93 ± 0.78	89.42 ± 1.97	89.42 ± 4.89	89.21 ± 11.02
Pixel Hits	99.45 ± 0.33	99.38 ± 0.89	99.36 ± 2.25	99.37 ± 5.59	100.00 ± 12.70
Tracking Hits	99.95 ± 0.34	99.96 ± 0.90	99.90 ± 2.27	99.84 ± 5.63	100.00 ± 12.70
Valid Muon Hits	97.40 ± 0.33	96.77 ± 0.88	97.01 ± 2.22	97.46 ± 5.53	96.77 ± 12.39
Muon χ^2	99.00 ± 0.34	98.59 ± 0.90	98.57 ± 2.28	99.02 ± 5.67	100.00 ± 12.91
Isolation	96.94 ± 0.33	89.80 ± 0.85	87.11 ± 2.09	86.66 ± 5.16	86.67 ± 11.61
p_T and $\lvert\eta\rvert$	91.67 ± 0.33	87.02 ± 0.87	88.69 ± 2.27	92.21 ± 5.80	91.35 ± 12.96
Total	44.12 ± 0.14	47.87 ± 0.43	50.55 ± 1.16	55.37 ± 3.13	55.88 ± 7.16

Figure 1: Pull distributions for fit with bad shape parameters

A set of toy experiments are carried out by generating toy samples according to the MC signal shape and refit using slightly wrong parameters. Each parameter is varied by 5%, 2% and 1% in both directions while keeping the other parameters floated. The pull distribution is shown in figure 1, while the induced bias is summarized in table 8.

The one parameter that we should be careful about is α_L.

Table 8: Bias induced by assuming bad signal shape parameters

4.3 Getting α_L from data

As shown above, among the four parameters the one with larger effect if the value assumed is wrong is α_L. Since the background shape is a falling spectrum and the α_L parameter in the signal shape controls the size of tail in the low-mass side, it is needed that we fix at least this parameter during the fit. Otherwise this parameter will adjust so that the background events are included in signal yield also, creating bias.

One way to extract the α_L is to require tight isolation on muons to get a high purity signal sample, and then fit to get the shape parameter. In MC signal sample fits are done varying isolation level, and the result summarized in figure 2. The shape depend only slightly on the isolation. Therefore it is fine to extract the shape parameter from data directly without using MC shape.

4.4 Simultaneous fit to all jet multiplicity bins

A maximum likelihood fit is performed simulatneously for all different jet counts, with the total likelihood written as

$$L = (Prefactor) \times \sum_i \{ \sum_{n_{jet}=1}^{n_{max}-1} \left((N_{S,n_{jet}} - N_{S,n_{jet}+1}) F_S(M_{ll}^i) + N_{B,n_{jet}} F_{B,n_{jet}}(M_{ll}^i) \right) \delta_{n_{jet},n_{jet}^i} + \left(N_{S,n_{max}} F_S(M_{ll}^i) + N_{B,n_{max}} F_{B,n_{max}}(M_{ll}^i) \right) \theta(n_{jet}^i - n_{max}) \},$$

where F_S is the signal PDF, constrained to be the same for all jet bins. The background PDF, $F_{B,n_{jet}}$, is not constrained to be the same for different jet bins, and the exponents are left floating in the fit. Each term (except the last) is constrained to be with the same exclusive jet bin through the Kronecker delta function $\delta_{n_{jet},n_{jet}^i}$. The

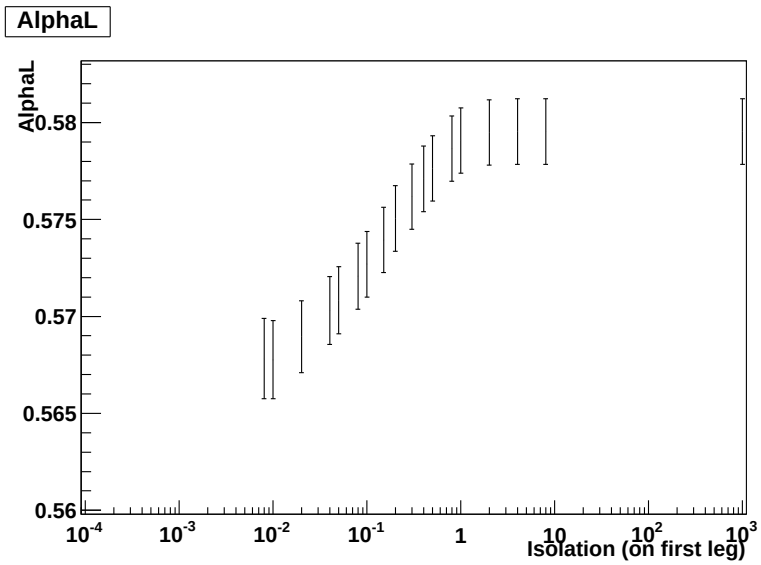

Figure 2: Shape parameter varying relative combined isolation level on muons.

last jet bin is inclusive, including all number of jets greater or equal to n_{max}, constrained by the step function $\theta(n^i_{jet} - n_{max})$. All the parameters for signal PDF are floated except α_L.

The assumption that signal shape is fixed across all jet multiplicity bins can be checked from the MC signal sample. Shape parameters for each jet multiplicity bin for different flavors of jets are summarized in table 9.

5 Data

Result of fit to data signal shape with tight isolation requirement is shown in table 10. The "tight isolation" here refers to 5% in units of relative combined isolation. Note that only the value of α_L is used in subsequent fits. All others are left floating.

Table 11 shows the extracted yields from the simultaneous fit for different jet flavors. The fit result together with ratio of N jets to (N+1) jets are shown in figures 3, 4, 5 and 6. Distribution of first 4 bins of jet multiplicity fits are shown in figures 7, 8, 9 and 10.

6 Systematic uncertainties

6.1 Jet energy correction uncertainty

One major systematic uncertainty arises from the jet energy scale correction uncertainties, which might affect the counting of jet multiplicity. In order to estimate the effect of jet energy correction, we followed the result from study of jet energy correction uncertainties (TODO: INSERT CITATION?):

1. 10% overall scale uncertainty for CaloJets, and 5% overall scale uncertainty for particle-flow jets
2. $2\% \times |\eta|$ pseudorapidity-dependent uncertainty for both types of jets
3. The two items above are assumed to add in quadrature.

Therefore we have artificially varied the jet energy by 1σ of each types (overall and eta-dependent) of uncertainties and redo counting for all events. After modifying the jet counts, the same simultaneous fit is performed for each case to extract signal yield. Difference of signal yield before and after adjusting energy scale is quoted as the systematics due to jet energy correction. The result is shown in figures 11 and 12 for CaloJets and PFJets, respectively.

Table 9: MC signal shape dependence across different jet multiplicities

Jet Counting	m	α_L	α_R	σ_L	σ_R
PFJets					
$N(\geq 0\ jets)$	938.78 ± 30.64	0.16 ± 0.41	1.21 ± 1.10	0.00 ± 0.00	
$N(\geq 1\ jets)$	140.18 ± 11.84	0.03 ± 0.18	1.18 ± 1.09	0.00 ± 0.00	
$N(\geq 2\ jets)$	25.05 ± 5.00	0.01 ± 0.11	0.95 ± 0.98	0.00 ± 0.00	
$N(\geq 3\ jets)$	4.54 ± 2.13	0.01 ± 0.11	0.41 ± 0.64	0.00 ± 0.00	
$N(\geq 4\ jets)$	0.90 ± 0.95	0.00 ± 0.00	0.13 ± 0.36	0.00 ± 0.00	
TrackJets					
$N(\geq 0\ jets)$	938.78 ± 30.64	0.16 ± 0.41	1.21 ± 1.10	0.00 ± 0.00	
$N(\geq 1\ jets)$	99.29 ± 9.96	0.03 ± 0.18	1.08 ± 1.04	0.00 ± 0.00	
$N(\geq 2\ jets)$	13.90 ± 3.73	0.01 ± 0.11	0.67 ± 0.82	0.00 ± 0.00	
$N(\geq 3\ jets)$	2.24 ± 1.50	0.00 ± 0.00	0.22 ± 0.47	0.00 ± 0.00	
$N(\geq 4\ jets)$	0.35 ± 0.59	0.00 ± 0.00	0.06 ± 0.24	0.00 ± 0.00	
CaloJets					
$N(\geq 0\ jets)$	938.78 ± 30.64	0.16 ± 0.41	1.21 ± 1.10	0.00 ± 0.00	
$N(\geq 1\ jets)$	211.96 ± 14.56	0.07 ± 0.26	1.19 ± 1.09	0.00 ± 0.00	
$N(\geq 2\ jets)$	43.27 ± 6.58	0.03 ± 0.16	1.02 ± 1.01	0.00 ± 0.00	
$N(\geq 3\ jets)$	8.63 ± 2.94	0.01 ± 0.11	0.52 ± 0.72	0.00 ± 0.00	
$N(\geq 4\ jets)$	1.81 ± 1.35	0.00 ± 0.00	0.21 ± 0.46	0.00 ± 0.00	
UncorrectedCaloJets					
$N(\geq 0\ jets)$	938.78 ± 30.64	0.16 ± 0.41	1.21 ± 1.10	0.00 ± 0.00	
$N(\geq 1\ jets)$	114.41 ± 10.70	0.05 ± 0.21	1.15 ± 1.07	0.00 ± 0.00	
$N(\geq 2\ jets)$	17.73 ± 4.21	0.01 ± 0.08	0.81 ± 0.90	0.00 ± 0.00	
$N(\geq 3\ jets)$	2.99 ± 1.73	0.01 ± 0.08	0.30 ± 0.55	0.00 ± 0.00	
$N(\geq 4\ jets)$	0.59 ± 0.77	0.00 ± 0.00	0.08 ± 0.29	0.00 ± 0.00	

Table 10: Shape parameters requiring one jet of different flavors fitting to data with tight isolation cut

	CaloJet	Uncorrected CaloJet	PF Jet	Track jet
m	90.83 ± 0.15	90.95 ± 0.18	91.04 ± 0.16	90.96 ± 0.20
α_L	0.522 ± 0.006	0.510 ± 0.008	0.488 ± 0.007	0.493 ± 0.009
α_R	0.441 ± 0.008	0.454 ± 0.009	0.448 ± 0.008	0.448 ± 0.011
σ_L	2.043 ± 0.115	2.225 ± 0.145	2.342 ± 0.129	2.237 ± 0.159
σ_R	2.205 ± 0.114	2.135 ± 0.138	2.071 ± 0.120	2.143 ± 0.154

Table 11: Data extracted yields

	CaloJet	Uncorrected CaloJet	PF Jet	Track jet
$N \geq 1$	3469 ± 75	2330 ± 52	2874 ± 63	1858 ± 50
$N \geq 2$	767 ± 33	416 ± 24	622 ± 28	311 ± 20
$N \geq 3$	159 ± 15	72 ± 10	116 ± 12	41 ± 8
$N \geq 4$	37 ± 7	11 ± 5	21 ± 6	5 ± 3
$N \geq 5$	6 ± 3	0 ± 0	2 ± 2	0 ± 0

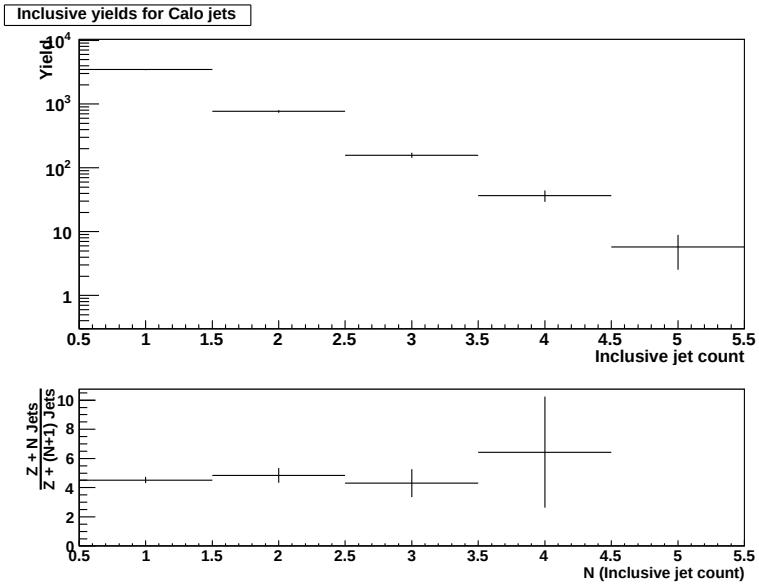

Figure 3: Summary of N/(N+1) jet ratio for calo jets

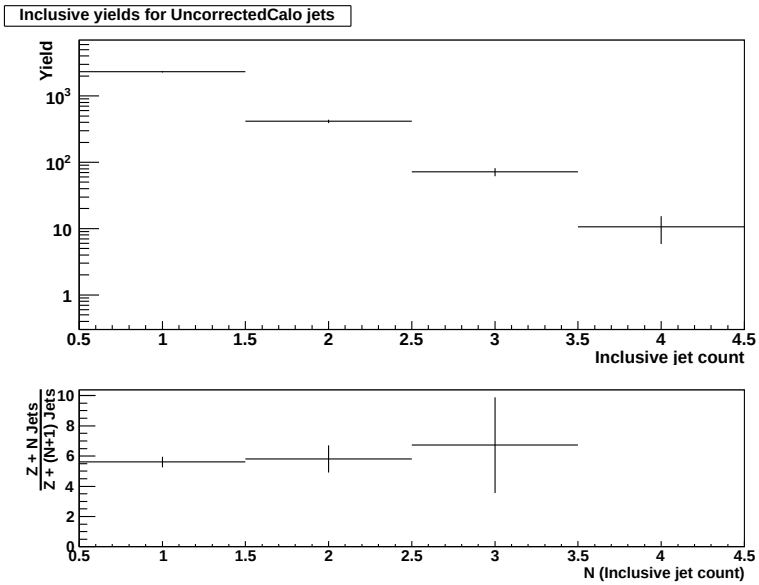

Figure 4: Summary of N/(N+1) jet ratio for uncorrected calo jets

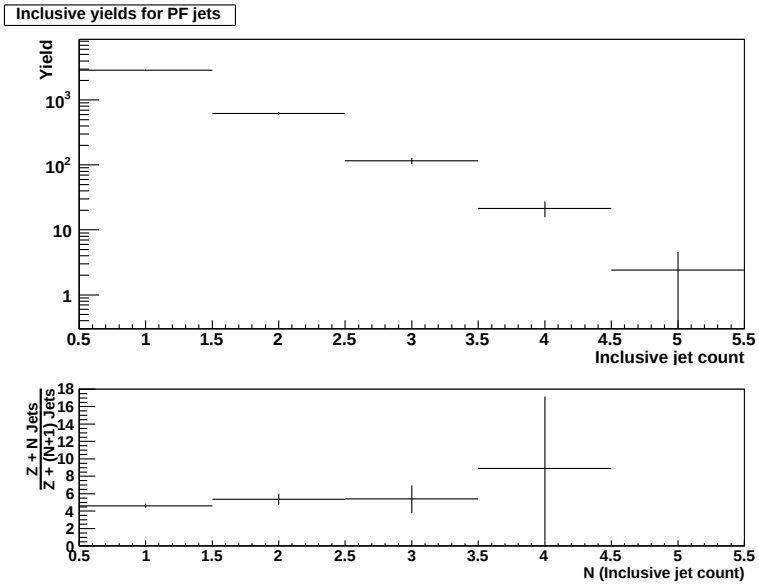

Figure 5: Summary of N/(N+1) jet ratio for particle-flow jets

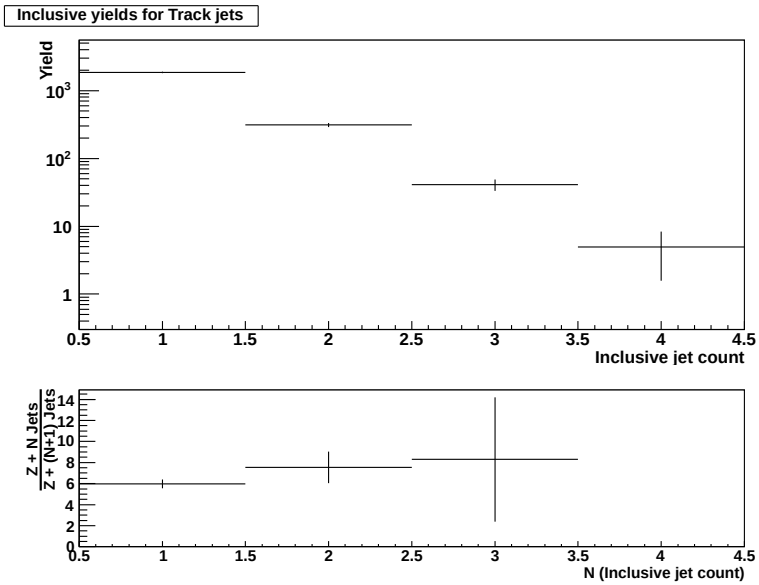

Figure 6: Summary of N/(N+1) jet ratio for track jets

Figure 7: First 4 jet multiplicity bins in calo jet counting

Figure 8: First 4 jet multiplicity bins in uncorrected calo jet counting

Figure 9: First 4 jet multiplicity bins in particle-flow jet counting

Figure 10: First 4 jet multiplicity bins in track jet counting

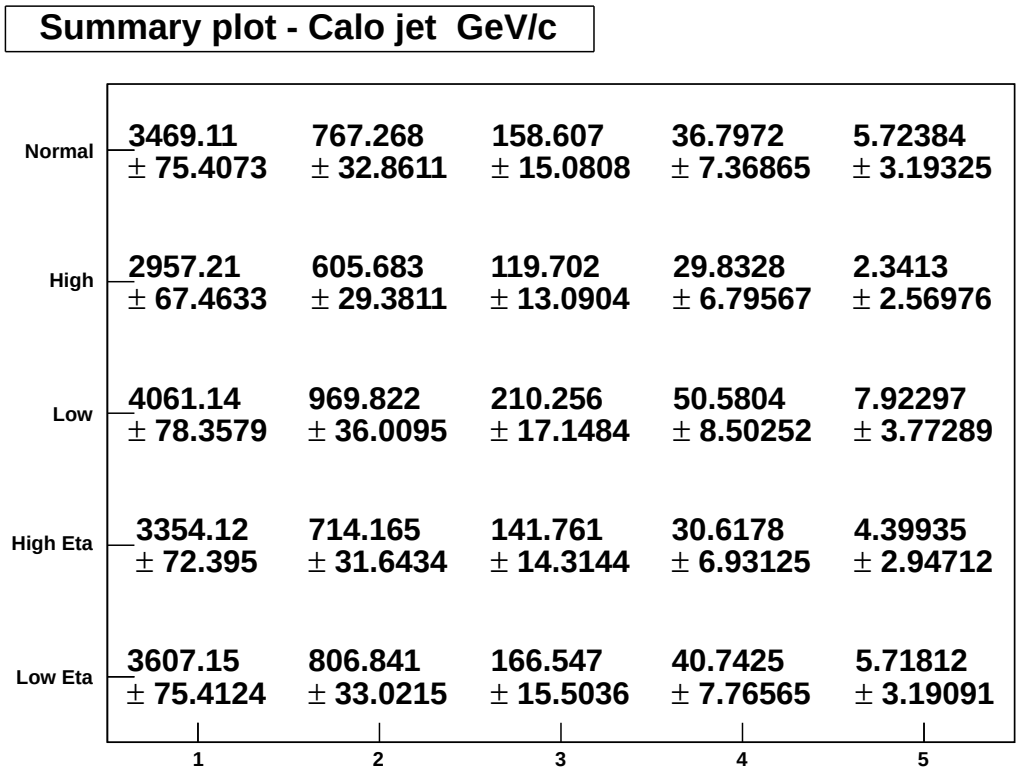

Figure 11: Jet energy scale uncertainty estimation for CaloJets

6.2 Background control sample

The background shape hypothesis is checked by inverting the isolation on the higher energy leg of muon. By comparing the QCD MC shape together with the isolation-inverted MC shape, we can see that the background shape is invariant to isolation requirement of the muon (TODO: CAN WE REALLY SEE?). Figure 13 shows the comparison between two MC shape and the isolation-inverted shape from data. The distributions are normalized. Indeed the distribution follows a falling distribution. Given the expected number of background events, an exponential should be able to describe the shape.

6.3 Bias on the simultaneous fit strategy

Toy! Will write this in on Sunday after all the toys finished running. (TODO)

7 Summary

We have presented the measurement of N/(N+1) jet ratio from the dimuon channel of Z0 boson events. The result on the ratio is within expectation.

...what can we say here? (TODO)

References

[1] **CMS AN-2001/100**, A. Author, B.Author *"Hmm"*

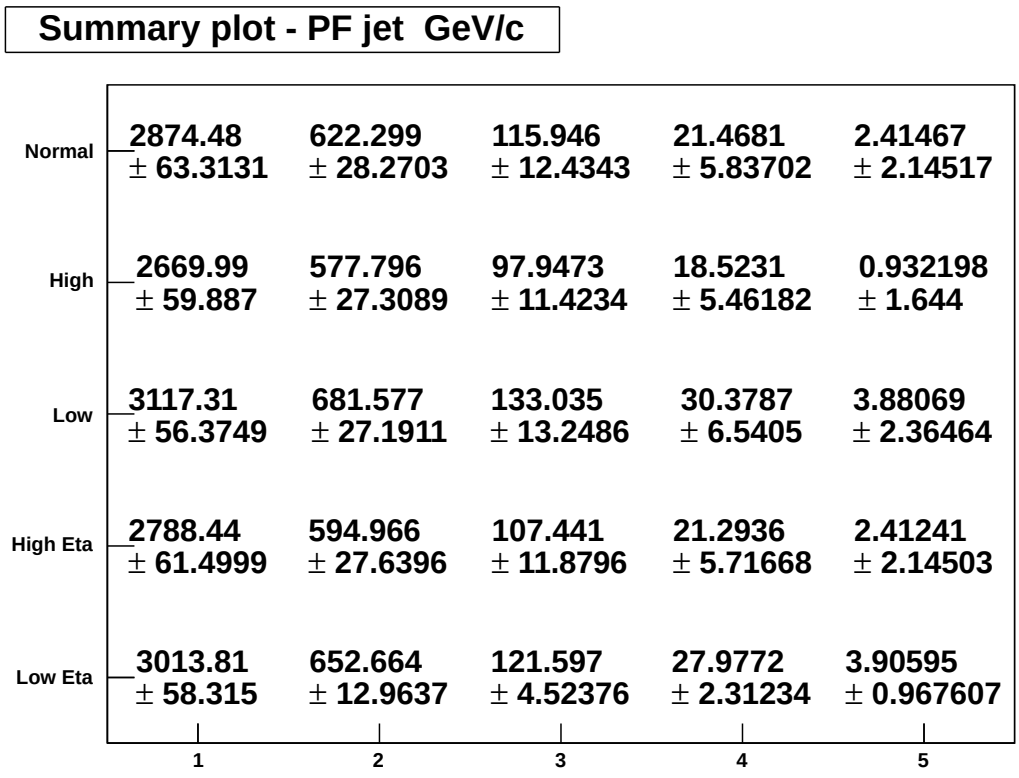

Figure 12: Jet energy scale uncertainty estimation for PF jets

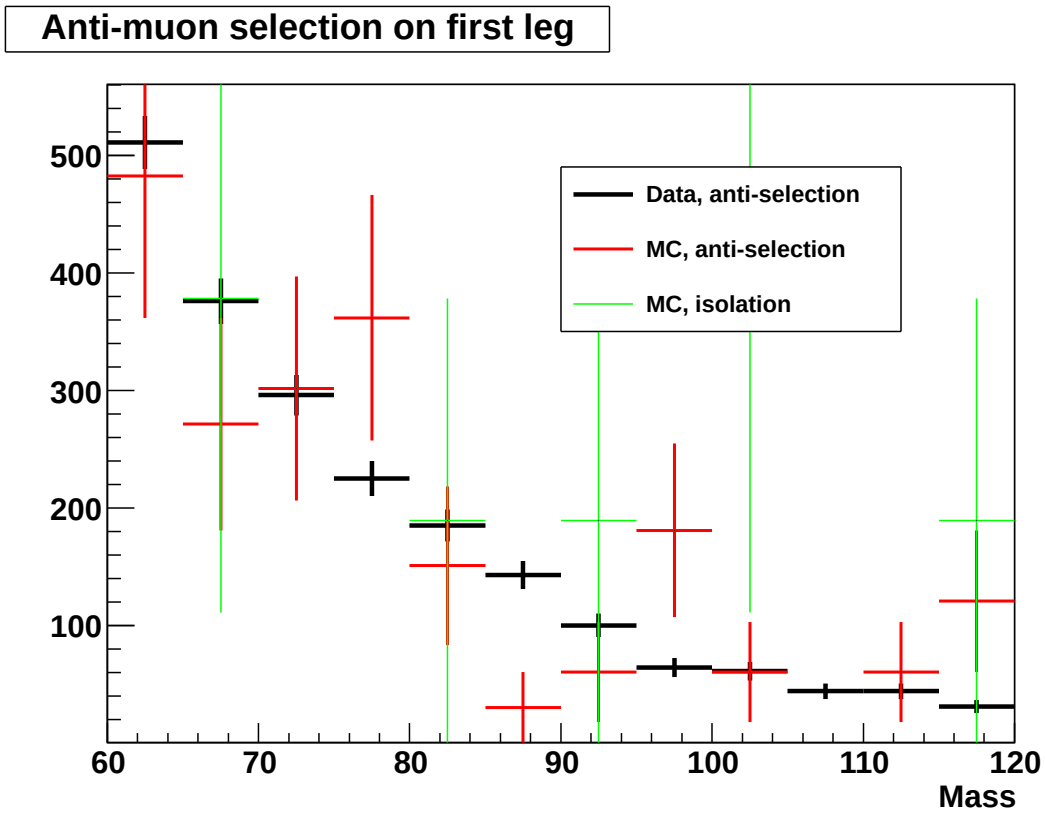

Figure 13: Background control sample with muon isolation inverted. The distributions are normalized to the same area.